SUPERPARAMAGNETIC NANOPARTICLES AND OPPOSITELY CHARGED POLYMERS: DESIGN OF NEW CONTRAST AGENTS FOR MAGNETIC RESONANCE IMAGING

J.–F. Berret[1], J.–P. Fortin[1], F. Gazeau[1], D. El Kharrat[2], O. Sandre[2]

[1] *Matière et Systèmes Complexes, UMR CNRS 7057, Université Denis Diderot Paris 7, 140 rue de Lourmel, 75015 Paris, France (jean-francois.berret@ccr.jussieu.fr)*
[2] *Laboratoire Liquides Ioniques et Interfaces Chargées, Université P. et M. Curie, 4, place Jussieu Boîte 51, F-75252 Paris Cedex 05, France*

Inorganic nanoparticles are currently used in a wide variety of material science and biomedical applications [1, 2]. For applications, inorganic particles often require to be concentrated, dried or mixed in various environments, transformations which sometimes result in their destabilization or precipitation. A broad range of techniques in chemistry and physical chemistry are now being developed to stabilize inorganic nanoparticles. Among these techniques, one can cite the adsorption of charged ligands or stabilizers on their surfaces [3], the layer-by-layer deposition of polyelectrolyte chains [4] or the surface-initiated polymerization resulting in a high-density polymer brushes [5]. In this letter we explore an alternative route. The nanoparticles are complexed by asymmetric block copolymers, where one block is charged and of opposite charge to that of the particles and the second block is neutral. We apply this concept to superparamagnetic Fe_2O_3 nanoparticles and show that the colloidal complexes resulting from this association have a remarkable stability in aqueous media. For these systems, magnetic resonance spin-echo measurements indicate a noticeable increase of the ratio between the transverse and longitudinal relaxivities R_2/R_1, which usually tests the efficiency of MR contrast agents. The results finally suggest that the polymer-nanoparticle aggregates could be used as T_2 contrast agents.

The block copolymers used for the complexation with nanoparticles were synthesized by controlled radical polymerization [6]. The anionic polyelectrolyte block is a poly (trimethylammonium ethylacrylate methylsulfate) chain and the neutral block is poly (acrylamide). In the following, this diblocks are abbreviated to as PTEA-*b*-PAM. Two molecular weights have been investigated, 5K-*b*-30K and 11K-*b*-30K corresponding to 19 and 41 monomers in the charged blocks and 420 for the neutral one. A detailed characterization of the polymers can be found in Ref. [7, 8]. The superparamagnetic nanoparticles (maghemite, γ-Fe_2O_3) were synthesized according to protocols described in [9, 10] and references therein. Magnetization and cryo-TEM measurements have shown that the γ-Fe_2O_3–nanoparticles are characterized by a size distribution well accounted for by a log-normal function, with an average diameter of 6.3 nm and by a polydispersity of 0.23 ± 0.03. Their surfaces are coated with citrate ligands which are negatively charged at neutral pH. In these conditions, the nanoparticles and the polyelectrolyte blocks are oppositely charged, and they can self-assemble in a mechanism based on electrostatics and charge compensation [7, 8, 11]. Polymer-nanoparticles complexes are obtained by mixing pure solutions prepared at the same concentration c and pH = 7. The mixing ratio X is defined as the volume of iron oxide sols relative to that of the polymer. In the present case, the quantity X is preferred (instead of the charge ratio) because the structural charges borne by the particles are not known. The concentrations in nanoparticles and polymers in the mixed solutions are $c_{pol} = c/(1 + X)$ and $c_{nano} = Xc/(1 + X)$, i.e., $X = 0$ denotes a pure polymer solution and $X = 1$
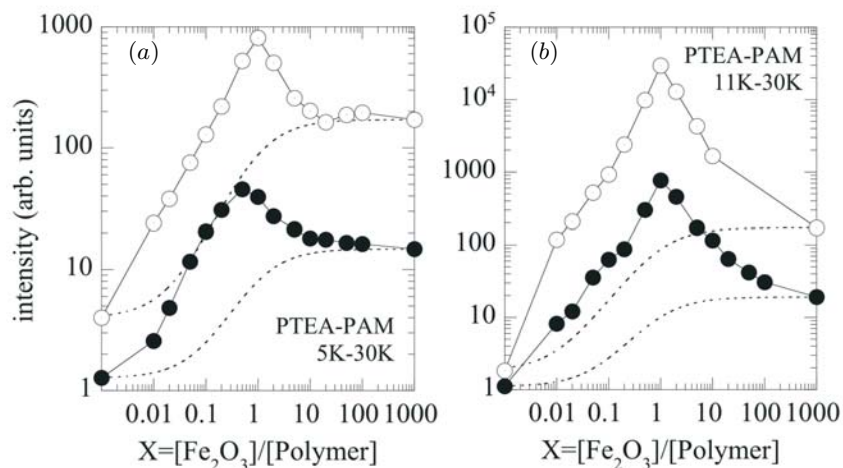
Fig. 1. Light scattering intensity $I_{90°}(X)$ measured for nanoparticle-polymer solutions for PTEA-*b*-PAM 5K-*b*-30K (left) and PTEA-*b*-PAM 11K-*b*-30K (right). The concentrations c are at $c = 0.2$ wt.% (closed symbols) and $c = 1$ wt.% (open symbols). The dotted lines represent the scattering intensities calculated assuming that the two components remain unassociated. These intensities are increasing with X because the molecular weight estimated for a nanoparticle ($M_w^{\mathrm{nano}} = 900000$ g · mol^{-1}) is much larger than that of the polymers.

a pure nanoparticle solution. For the mixed solutions, no phase separation or precipitation have been observed during or after the mixing.

In order to follow the formation of mixed nanoparticle-polymer complexes, we have performed light scattering measurements in a 90°-configuration for two series of solutions at $c = 0.2$ wt.% and $c = 1\%$. Figs. 1a and 1b display the scattered intensities $I_{90°}(X)$ for PTEA-*b*-PAM 5K-*b*-30K and PTEA-*b*-PAM 11K-*b*-30K, respectively with X ranging from 10^{-2} to 100. With these notations [12], a solution at $c = 1\%$ and $X = 1$ corresponds to iron molar concentration [Fe] = 63.4 mmol · l^{-1}. Because of the absorption of the incident light due to the deeply colored iron oxide sols, the transmittance at 633 nm was measured by UV-visible spectrometry for each solution and the scattered intensities were corrected, accordingly. The scattered intensity $I_{90|circ}(X)$ is found to pass through a maximum at $X_P \sim 1$ for the four series of solutions (Figs. 1). For dispersed macromolecules and colloids, it is known that the scattered intensity extrapolated at zero concentration and zero scattering angle goes as $I_{\theta \to 0}(c \to 0) \sim cM_{W,\mathrm{app}}$, where $M_{W,\mathrm{app}}$ is the weight-averaged molecular weight of the scattering entities. As X is varied in Figs. 1, the total concentration c remains constant and thus, according to the above relationship, the data are indicative of the apparent molecular weight of the aggregates dispersed in solution. Also displayed in Figs. 1 as dotted lines are the scattering intensities of mixed solutions computed if the particles and the polymers remain unassociated. We interpret the excess intensities above the calculated ones as an evidence of the formation of polymer-nanoparticle aggregates. There, $X_P < 1$ corresponds to the range, where the polymer is the majority component, and we assume that all the nanoparticles participate to the aggregates. For $X_P > 1$, the nanoparticles are in excess and again we assume that all the polymers are consumed to build the mixed colloids. Using the molecular weights of the single components, the number of polymers per particle at X_P can be estimated. We found $n^{\mathrm{pol}}/n^{\mathrm{nano}} \sim 20$ for the two sets of systems.

Dynamic light scattering performed on the solutions at $c = 0.2$ wt.% confirms the hypothesis of the formation of mixed aggregates. Fig. 2 (left) displays the X-dependence of the average hydrodynamic diameter D_H. Here D_H is calculated

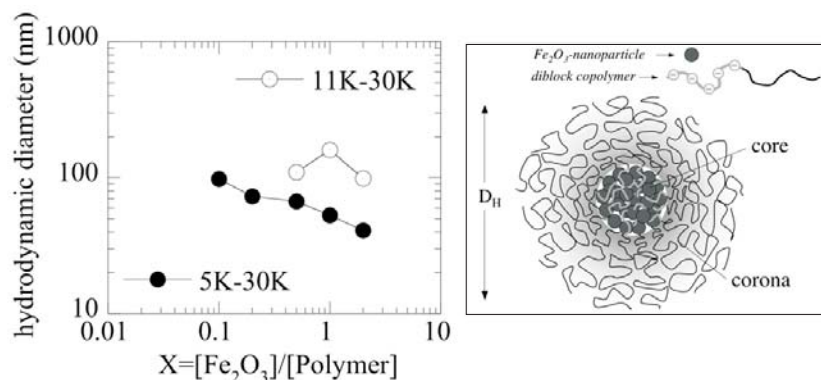*Fig. 2.* Left: X-dependence of the average hydrodynamic diameter D_H for $c = 0.2$ wt.% mixed solutions. $D_H^{pol} = 11$ nm [8] and $D_H^{nano} = 8.7$ nm for the individual components. Right: Microstructure assumed for the mixed polymernanoparticle complexes. The electrostatic self-assembly giving rise to this structure is based on the complexation between the charges located on the surface of the anionic particles and along the cationic block.

from the autocorrelation function of the scattered light at different angles. For $X = 0.1$–2, D_H is of the order of 100 nm for PTEA-b-PAM 11K$-b$-30K and it decreases slightly for the 5K$-b$-30K polymer. D_H-values well above those of the individual components ($D_H^{pol} = 11$ nm [8] and $D_H^{nano} = 11$ nm) suggest again the formation of mixed aggregates.

In conclusion of the light scattering study, we propose to draw an analogy between the present results and those obtained by complexation of the same cationic-neutral copolymers with surfactant micelles [7, 8] and with yttrium-based inorganic particles [12]. The results shown here are qualitatively similar to those discussed in these papers. Fig. 2 (right) shows a schematic representation of a mixed aggregate. It comprises a core of densely packed nanoparticles and a corona made of the neutral blocks. Note that according to the present model, the size of the core is much smaller than the hydrodynamic diameter shown in Fig. 2 (left).

Relaxometry has been used to measure the longitudinal (T_1) and transverse (T_2) relaxation times of the proton Larmor frequency for the polymer-nanoparticle solutions described previously. The measurements were performed using a Minispec PC120 spectrometer (Brucker) operating with a magnetic field of 0.47 T (corresponding to 20 MHz for the proton Larmor frequency) and at $T = 37°$C. The sequences and procedures for the determinations of the relaxation times are described in Ref. [10]. Figs. 3a and b show the inverse relaxation times $1/T_1$ and $1/T_2$ for PTEA-b-PAM solutions prepared at $X = 0.5$ and at $c = 0.2$ wt.%. The two solutions are characterized by hydrodynamic diameters $D_H \sim 70$ nm (for 5K-b-30K) and $D_H \sim 110$ nm (for 11K-b-30K). In order to allow the detection of the inversion-recovery dynamics and of the echoes with the spectrometer, the solutions were diluted by a factor 10 to 1000 and experiments were carried out for iron molar concentrations comprised between 0.5 and 6 mmol$\cdot$l^{-1}. It was checked that the size and microstructure of the polymer-nanoparticle complexes were not modified under dilution. In Figs. 3, the inverse relaxation times are found to vary linearly with the concentration, according to $1/T_{1,2}([\text{Fe}]) = R_{1,2}[\text{Fe}] + 1/T_{1,2}^0$, where $R_{1,2}$ are the longitudinal and transverse relaxivities [13]. The intercepts $1/T_{1,2}^0$ are the water diamagnetic constants.

As shown in earlier reports, the values of the relaxivities are intrinsic properties of the aggregates dispersed in solutions. Here, we found that R_2 is increased when the nanoparticles are associated, whereas R_1 remains almost unaffected. Within the samples investigated by relaxometry in this work, the ratio R_2/R_1
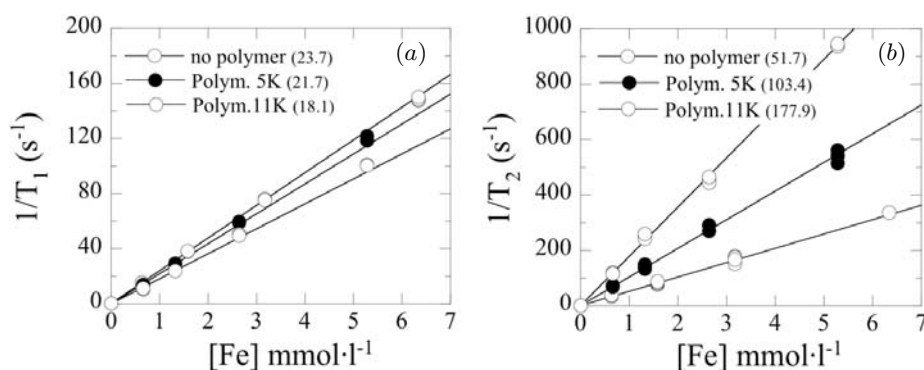
391

Fig. 3. Inverse longitudinal and transverse relaxation times $1/T_1$ and $1/T_2$ for systems prepared at $X = 0.5$ and at $c = 0.2$ wt.% as a function of the iron molar concentration [Fe]. The mixed solutions are characterized by an hydrodynamic diameter $D_H \sim 70$ nm (for 5K-*b*-30K) and $D_H \sim 110$ nm (for 11K-*b*-30K). The inverse relaxation times for the pure ferrofluid solution are also included for comparison. The relaxivities R_1 and R_2 (derived from the slopes of the straight lines) are indicated in parenthesis.

varies from 2.2 for the single particles ($D_H^{\mathrm{nano}} = 11$ nm) to 10.5 for the largest aggregates obtained so far, that is for $c = 1$ wt.%, $X = 1$ ($D_H \sim 200$ nm, data not shown in Figs. 4). Such values indicate that the polymer-nanoparticle aggregates could be used as T_2 contrast agents. It is interesting to compare here these results with those obtained with other types of magnetic particles and aggregates [9, 10, 13, 14, 15]. For submicrometric unilamellar vesicles loaded with ferrofluid, Billotey *et al.* [9] and Martina *et al.* [10] have shown the same variation of the relaxivity ratio R_2/R_1 with increasing iron loading. Recently, Manuel–Perez *et al.* [14, 15] have found that the self-assembly of 50 nm-particles induced by the presence of a virus yields an increase in the transverse time T_2, and thus a decrease of the related relaxivity R_2. Although this system is close to the present one, the results by Manuel–Perez *et al.* differ from the data shown in Fig. 4.

In conclusion, the controlled association of superparamagnetic particles has been realized by electrostatic self-assembly using block copolymers. We have shown that the mixed complexes have an excellent colloidal stability due to the neutral corona, and that they could be used as T_2-contrast agents in magnetic resonance.

REFERENCES

1. J.A. LEWIS. *J. Am. Ceram. Soc.*, vol. 83 (2000), pp. 2341–2359.
2. O. SPALLA. *Curr. Opin. Colloid Interface Sci.*, vol. 7, (2002), pp. 179–185.
3. S. DESSET *et al.* *Langmuir*, vol. 17, (2001), pp. 6408–6418.
4. F. CARUSO *et al.* *Science*, vol. 282 (1998), pp. 1111–1114.
5. H. OHNO *et al.* *Macromolecules*, vol. 35 (2002), pp. 8989–8993.
6. M. DESTARAC *et al.* *Macromol. Rapid Commun.*, vol. 23 (2002), p. 1049.
7. J.–F. BERRET *et al.* *J. Phys. Chem. B*, vol. 107 (2003), pp. 8111–8118.
8. J.–F. BERRET *et al.* *Macromolecules*, vol. 37 (2004), pp. 4922–4930.
9. C. BILLOTEY *et al.* *Magn. Res. Med.*, vol. 49, (2003), pp. 646–654.
10. M.–S. MARTINA *et al.* *Radiology* (2005). (in press.)
11. J.–F. BERRET *et al.* *Eur. J. Phys. E*, vol. 9 (2002), pp. 301–311.
12. K. YOKOTA *et al.* *Europhys. Lett.*, vol. 69 (2004), pp. 284–290.
13. P. GILLIS, S.H. KOENIG. *Magn. Res. Med.*, vol. 5 (1987), pp. 323–345.
14. J.M. PEREZ *et al.* *J. Am. Chem. Soc.*, vol. 124 (2002), pp. 2856–2857.
15. J.M. PEREZ *et al.* . *J. Am. Chem. Soc.*, vol. 125 (2003), pp. 10192–10193.